Bridging the Seismic Monitoring Gap around Saba, St. Eustatius, and St. Maarten in the Caribbean Netherlands: The NA Network

Reinoud Sleeman*[1] and Elske de Zeeuw-van Dalfsen[1]

ABSTRACT

The seismic network NA (Caribbean Netherlands Seismic Network) in the Caribbean Netherlands is deployed by the Royal Netherlands Meteorological Institute (KNMI) to monitor local seismicity around Saba, St. Eustatius, and St. Maarten, and to contribute data to regional earthquake and tsunami warning monitoring systems. The network currently comprises 11 broadband seismometers that record data processed in real time at KNMI, using SeisComP and a coincidence trigger. Between January 2017 and April 2022, we detected and located 241 earthquakes within 150 km distance from the center of the network with magnitudes from 0.4 to 6. Reanalysis of data before 2017 revealed a swarm of 22 tectonic earthquakes in 2008, within 15 km distance west of Saba with magnitudes between 2.3 and 4 at shallow (5–10 km) depths. The complex seismic velocity structure, the large lateral velocity inhomogeneities in the subduction zone, and the elongated setup of the regional seismic network are challenges for the earthquake location process. We compare our results with the U.S. Geological Survey catalog and find differences that fall within the uncertainty ellipses for 85% of the earthquakes. The NA network is an important contribution to the regional earthquake and tsunami warning monitoring systems, and for studying subduction and volcanic processes in the Lesser Antilles arc.

KEY POINTS

- KNMI deploys a seismic network for volcano, tsunami, and earthquake monitoring in the Caribbean Netherlands.
- The network increased from 3 to 11 BB seismometers during 2015–2022.
- We detect previously unnoticed earthquakes within 150 km distance from our network down to magnitude 0.4.

INTRODUCTION

Both Saba and St. Eustatius in the Caribbean Netherlands (Fig. 1) are part of the Lesser Antilles volcanic arc, which is the surface feature of the subduction of the American plates under the Caribbean plate. The arc is prone to a multitude of geophysical hazards, for example, earthquakes (e.g., Zimmerman *et al.*, 2022), volcanic eruptions (Lindsay and Robertson, 2018), and tsunamis (Proenza and Maul, 2010). Monitoring of these phenomena is essential for hazard mitigation and disaster management purposes. In 2006, the Royal Netherlands Meteorological Institute (KNMI) started the deployment of a broadband (BB) seismic network (de Zeeuw-van Dalfsen and Sleeman, 2018) with the installation of three BB seismometers (Table 1), on Saba, St. Eustatius, and St. Maarten to monitor the seismicity on and around these islands. Both Saba and St. Eustatius host an active but quiet stratovolcano: Mt. Scenery on Saba and The Quill on St. Eustatius. In 2010, Bonaire, St. Eustatius, and Saba became special municipalities of the Netherlands. This enhanced the demand for improved volcano monitoring, and the detection and monitoring capabilities of earthquakes on and around these islands.

The KNMI Department "Research and Development of Seismology and Acoustics" was tasked with this responsibility, and, in 2015, the seismic monitoring network on both Saba and St. Eustatius was expanded with three additional seismometers on each island. The monitoring network, however, was still not commensurate with the threats posed by the volcanoes (de Zeeuw-van Dalfsen and Sleeman, 2018). To overcome this "monitoring gap" a financial investment by the government was realized, which enabled a further expansion of the network

1. KNMI, De Bilt, Netherlands, https://orcid.org/0000-0002-1928-5056 (RS); https://orcid.org/0000-0003-2527-4932 (EdZ-vD)

*Corresponding author: sleeman@knmi.nl

Cite this article as Sleeman, R., and E. de Zeeuw-van Dalfsen (2022). Bridging the Seismic Monitoring Gap around Saba, St. Eustatius, and St. Maarten in the Caribbean Netherlands: The NA Network, *Bull. Seismol. Soc. Am.* **113**, 143–156, doi: 10.1785/0120220126

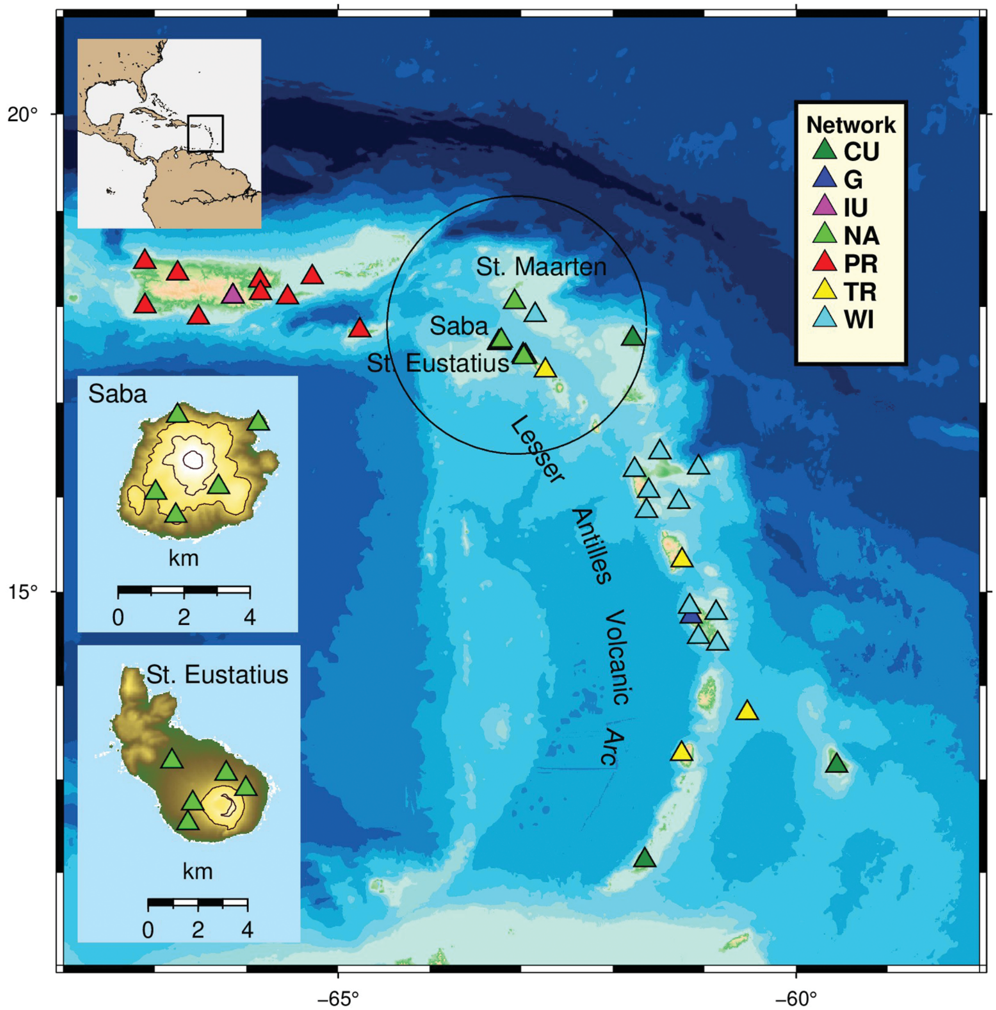

Figure 1. Geographical location of Saba, St. Eustatius, and St. Maarten at the northern part of the Lesser Antilles volcanic arc in the Caribbean (inset top left). Colored triangles are seismic stations from the NA (KNMI, 2006) and adjacent networks contributing waveform data to our automatic earthquake detection system. The NA network is deployed on Saba (five seismometers; inset left middle), St. Eustatius (five seismometers; inset left bottom), and St. Maarten (one seismometer). The area of focus for this work is indicated with the circle, which has a radius of 150 km around the center of the NA network. Background shows a bathymetry map (General Bathymetric Chart of the Oceans [GEBCO]). Adjacent networks are: CU (Caribbean U.S. Geological Survey [USGS] Network; Albuquerque Seismological Laboratory/U.S. Geological Survey [ASL/USGS], 2006); G (GEOSCOPE network; Institut de Physique du Globe de Paris [IPGP]& École et Observatoire des Sciences de la Terre de Strasbourg [EOST], 1982); IU (Global Seismograph Network, Albuquerque Seismological Laboratory/U.S. Geological Survey [ASL/USGS], 1988); PR (Puerto Rico Seismic Network; University of Puerto Rico, 1986); TR (Eastern Caribbean Seismograph Network; University of the West Indies, Seismic Research Center Trinidad [UWI-seismic], 1965); and WI (West Indies French Seismic Network; Institut de Physique du Globe de Paris [IPGP], 2008).

between 2018 and 2022, during which three more BB seismometers were installed.

The present regional seismic networks (CU, G, IU, NA, PR, TR, and WI; for locations and abbreviations see Fig. 1) complement each other in the monitoring of the volcanic arc. However, the limited geographical coverage and aperture of permanent seismic networks around Saba and St. Eustatius make it difficult to systematically detect and locate earthquakes accurately in this region. Sources of earthquake information are the International Seismological Center (ISC), U.S. Geological Survey (USGS), European–Mediterranean Seismological Center (EMSC), and the Seismic Research Center of the University of the West Indies (SRC-UWI). The building of a single, unified catalog for the Lesser Antilles, however, is a challenging task and the levels of completeness and accuracy are limited. A unified regional earthquake location catalog of known tectonic earthquakes in the Lesser Antilles subduction zone for 1997–2012 was produced by Massin *et al.* (2021). They estimated a magnitude of completeness for the region around Saba and St. Eustatius of 3.5 for the subduction zone and of 3.2 for crustal tectonic events, during 2000–2012. This is corroborated by our observation that no earthquakes within 60 km distance from Saba with magnitudes below magnitude ~3 are reported in the USGS catalog (Fig. 2a) between 2017 and 2021. As a consequence, small tectonic and/or volcanic earthquakes on Saba and/or St. Eustatius could have been unnoticed in the past.

DSL, digital subscriber line; VSAT, very small aperture terminal.

SRC-UWI deploys a volcanological and seismological surveillance network (TR, Fig. 1) since 1953 (Dondin *et al.*, 2019) with the mission to monitor 17 of the 21 active volcanoes of the Lesser Antilles volcanic arc. From 1992 to 2004, SRC-UWI operated one seismometer at the summit of Mt. Scenery (Roobol and Smith, 2004). Between 2008 and 2014, the Caribbean seismic network deployed by the Institut de Physique du Globe de Paris (WI, Fig. 1), focussing on Guadeloupe and Martinique, was modernized in collaboration with SRC-UWI. During this time, significant technical advances were made in the setup of new BB seismic stations (Anglade *et al.*, 2015), which further improved the detection capability in the region. The use of VSAT technology reinforces the WI network further, especially in terms of data availability

TABLE 1
Current Configuration and Characteristics of the NA Network (Status: May 2022)

Code	Operating (yyyy/mm/dd)	Datalogger	Sensor	Power	Communication	General Site Description and Characteristics
SABA	2006/10/31–	Q330	STS-2	Grid	DSL	In corner of temperature controlled room in concrete building
SABN	2021/04/04–	Q330S+	STS-2.5	Solar	VSAT	Concrete vault on volcanic deposits
SABQ	2015/10/05–	Q330S+	STS-2.5	Grid	DSL	In corner of temperature controlled room in concrete building
SABV	2015/07/17–2018/12/05	Q330S+	STS-2.5	Grid	DSL	In corner of temperature controlled concrete out-building
SABW	2015/07/17–	Q330S+	STS-2.5	Grid	DSL	In corner of temperature controlled room in concrete building
SABY	2021/01/19–	Q330S+	STS-2.5	Grid	DSL	Under staircase of temperature controlled building
SEUB	May 2022	Q330S+	STS-2.5	Solar	3G/4G	Concrete vault on soil
SEUG	2014/01/28	Q330S+	STS-2.5	Grid and solar	VSAT	Concrete vault on gently sloping soil
SEUH	2021/06/23	Q330S+	STS-2.5	Solar	VSAT	Concrete vault on concrete slab in soil
SEUS	2006/10/29	Q330S+	STS-2	Grid	DSL	In corner of temperature controlled storage room in concrete building
SEUT	2014/01/28	Q330	STS-2.5	Grid	DSL	In corner of temperature controlled room in concrete building
SMRT	2006/10/30	Q330	STS-2	Grid	DSL	Temperature controlled room in concrete building

during and after natural hazards. The Puerto Rico Seismic Network (PR, Fig. 1), operated by University of Puerto Rico (UPR), is located west of Saba and covers Puerto Rico, the Dominican Republic, and the U.S. and British Virgin Islands. The NA network aims to bridge the seismic monitoring gap in the volcanic arc around Saba and St. Eustatius.

The ongoing subduction process is the source of geophysical activity, for example, earthquakes and volcanic eruptions. This natural process cannot be prevented, but adequate monitoring can provide timely warning to local governments and populations. To enhance both monitoring and research capabilities, the availability of seismic data is crucial. Data from the NA network are openly available from KNMI and the European Integrated Data Archive (EIDA; Strollo *et al.*, 2021) at ORFEUS. Waveform data from the NA stations are used by the Pacific Tsunami Warning Center for tsunami warning services.

Besides the very important societal functions, data from the seismic network are also used for research. For example, Bie *et al.* (2019) used data from the NA stations to build a unified velocity model for the Lesser Antilles arc, and temporal changes in subsurface seismic velocity under Saba and St. Eustatius were investigated by applying seismic interferometry (Sleeman and de Zeeuw-van Dalfsen, 2020).

In this article, we present the current status of the NA network in the Caribbean Netherlands and provide details on a coincidence trigger to detect earthquake signals. We provide details of our catalog that currently holds 241 manually reviewed earthquakes that occurred between January 2017 and April 2022 less than 150 km from the center of the network. Finally, we evaluate a swarm of 22 manually reviewed, tectonic earthquakes within 15 km distance west of Saba that took place in 2008, and three more comparable earthquakes in 2013 and 2014.

THE NA SEISMIC NETWORK

The seismic network NA (see Data and Resources) currently comprises 11 permanent BB seismometers (Table 1). In 2006, single stations were installed on Saba (SABA), St. Eustatius (SEUS), and St. Maarten (SMRT). Additional seismometers were installed in 2014 and 2015 on Saba (SABQ, SABV, and SABW) and St. Eustatius (SEUG and SEUT). Station SABV was moved in 2018, after damage by lightning, to another location and renamed SABY. All these stations except SEUG are located in buildings with regulated temperature, power supply, and Internet availability through leased lines. SEUG is placed in a small concrete vault on a gentle slope, without air temperature regulation. In 2021 and 2022, the network was further expanded by stand-alone, off-grid seismometers on Saba (SABN) and St. Eustatius (SEUH and SEUB). These sites are equipped with solar panels for power supply and VSAT (SABN and SEUH) or mobile network (SEUB) for data transmission. The off-grid seismometers are placed in a concrete vault similar to SEUG, made of a 1 × 1 m horizontal base plate and vertical walls of 40 cm height, all constructed from concrete with a thickness of 10 cm. The vault is covered with a stainless steel lid. The base plate is anchored into the ground using 60 cm deep steel pipes or rebar. Walls are protected by piled rocks. All dataloggers are configured to produce three data streams (HH: 100 samples per second, BH: 40 samples per second, and LH: 1 samples per second) for each component (Z, N, and E) representing the ground velocity in vertical, north–south, and east–west directions. We have chosen to deploy (nearly) identical equipment at all sites to allow for efficient maintenance and interchangeability. We selected instruments that have proven to operate reliably in the Netherlands for almost 20 yr (see Data and Resources).

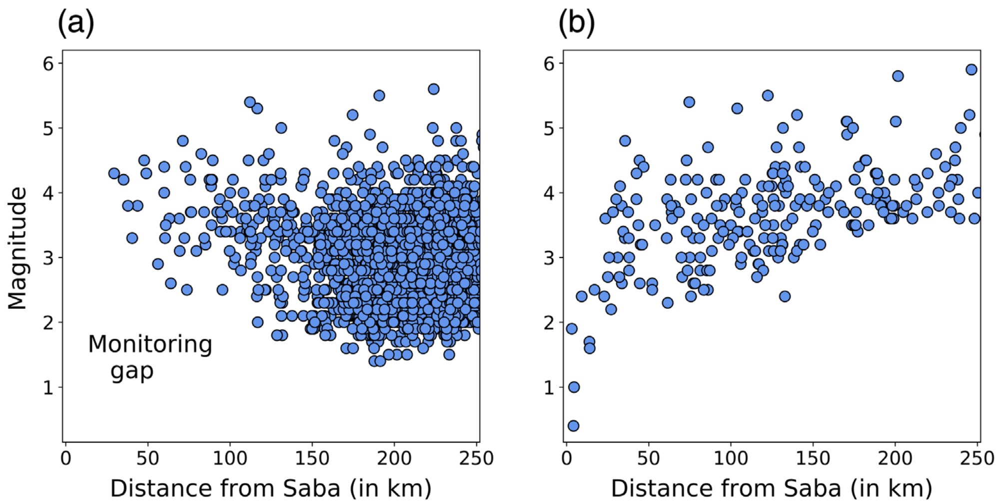

Figure 2. Magnitude–distance distribution of earthquakes reported by (a) USGS and (b) Royal Netherlands Meteorological Institute (KNMI) from 2017 to 2021 within 2° distance from seismic station SABA on Saba. Two **M** 2.5 events reported by USGS (14 March 2017 06:04:35 and 22 May 2017 09:01:02) at distances of 15.7 and 40.8 km from Saba are discarded, as no earthquake signals are detectable in the NA waveform data for these events. Note that beyond 150 km distance the number of earthquakes detected and located by USGS increases due to the vicinity of the PR network and incompleteness of our catalog. The color version of this figure is available only in the electronic edition.

SEISMICITY NEAR SABA

Because of lack of data in the past, local seismicity studies around Saba, St. Eustatius, and St. Maarten are very limited. However, a minor earthquake swarm of 60 detected earthquakes near Saba in June 1992 was studied by Ambeh and Lynch (1995). The detection threshold lowered significantly after SRC-UWI installed a single seismometer on Saba during the swarm (Ambeh and Lynch, 1995). For 15 earthquakes, hypocentral parameters could be determined with magnitudes ranging from 2.9 to 4.5. Their hypocenters, at depths between 10 and 16 km, show a distribution in the west-southwest–east-northeast direction, at about 2–20 km west from Saba and are considered to have a tectonic rather than a volcanic origin.

Another earthquake swarm was detected by the single SRC-UWI seismometer on Saba from May 1995 to April 1997. The activity peaked in December 1996 when 64 earthquakes were recorded (Roobol and Smith, 2004). At the time this activity was attributed by Roobol and Smith (2004) to a mild volcano-seismic crisis, as it coincided with an apparent temperature increase of the hotspring on Saba. The location of these earthquakes could not be identified but must have been within the vicinity of Saba.

In January 2008, multiple earthquakes were felt by the population of Saba and recorded by the single NA seismometers on Saba, St. Eustatius, and St. Maarten. On 14 January 2008 at 14:32:09, an **M** 4.0 earthquake occurred west of Saba at a depth of 7 km, followed by an **M** 3.9 earthquake nearly 2 min later. The ISC also reported 11 earthquakes that occurred in January 2008 just west of Saba. These events are in the vicinity of the earthquake swarm of 1992. The repeated earthquake swarm activity west of Saba warrants special attention to the analyses of all NA data for earthquakes in this area.

DETECTION AND PROCESSING

Our automated earthquake detection system is built upon SeisComP (see Data and Resources). In our configuration, waveform data from adjacent seismic networks (Fig. 1) are collected in real time to enable detection of regional earthquakes. Besides the limited station coverage in the area, the lack of a well-constrained 1D velocity model for the Lesser Antilles arc contributes to the uncertainties in earthquake parameters. A reference 1D model for the Lesser Antilles region proposed by Bie *et al.* (2019) may improve these uncertainties. However, first tests using this model do not yet show a distinct improvement, and therefore results in our work are based on the IASPEI91 velocity model (Kennett and Engdahl, 1991), in conjunction with LocSat (Bratt and Naggy, 1991) implemented in SeisComP.

Local tectonic earthquakes with magnitudes below 3 and within tens of kilometers distance from Saba and St. Eustatius, and/or volcanic earthquakes under Mt. Scenery or the Quill are not located by other seismic networks in the region (Fig. 2). In addition, small earthquakes that are only recorded by the network on Saba, or by the network on St. Eustatius, may not be detected and located by SeisComP due to a minimum of channels that is required in the detection and location process. To overcome this limitation and detect these small earthquakes with our NA network, we apply a network coincidence trigger.

A coincidence trigger searches for the temporal overlap of individual detections of (seismic) energy in a set of data streams. In our implementation, detections in a data stream are obtained by applying (1) a band-pass filter between 3 and 8 Hz and (2) a recursive short-term average (STA) over long-term average (LTA) filter (Havskov *et al.*, 2012). Parameters for the STA/LTA filter are: STA window length of 1 s, LTA window length of 9 s, and thresholds for start and end of the STA/LTA trigger of 3 and 1. The number of detections are counted in the time window defined by the start and the end of the STA/LTA trigger. If this number exceeds a certain threshold, a coincidence trigger is declared. The availability of data streams may vary over time (e.g., due to

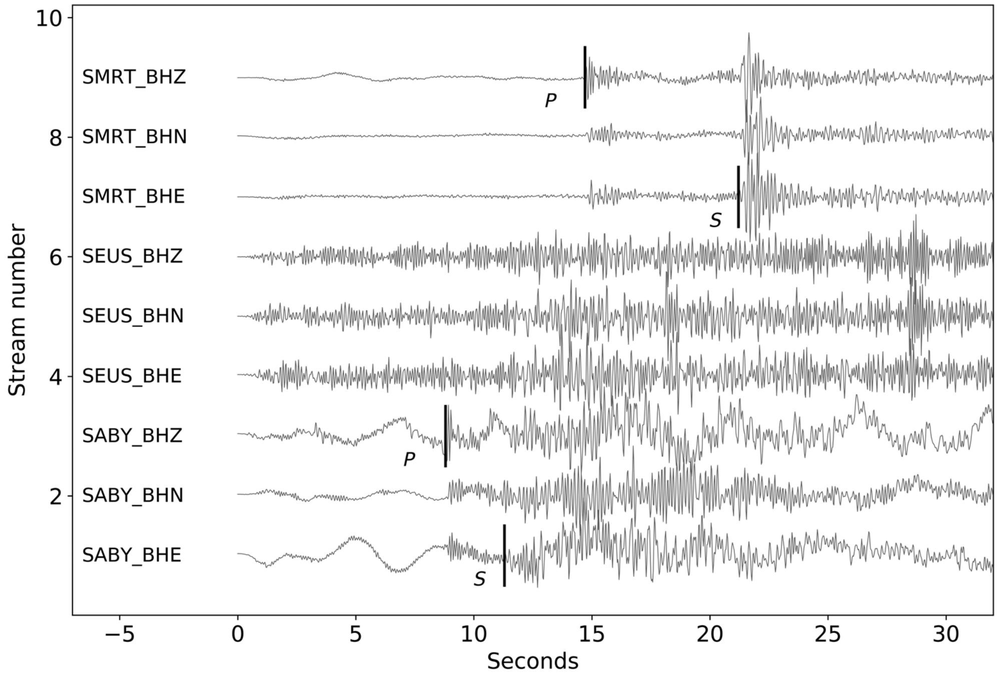

Figure 3. Recordings of an earthquake (25 November 2021 16:34:35 UTC) at a distance of 12 km east of Saba (depth 10 km, magnitude 1.7), detected by the coincidence trigger applied to the data from the seismometers on Saba. Data are shown from St. Maarten (SMRT), St. Eustatius (SEUS) and Saba (SABY). Note that this earthquake was too small to be detected by SeisComP and the seismometers on St. Eustatius at about 22 km distance. All traces are scaled to their maximum amplitude. Manual *P* and *S* picks are indicated with the vertical lines.

technical issues), and we set the threshold to 9 when 12 data streams or less are available and to 12 when more than 12 data streams are available.

For the 2007–2016 period, we focused on the detection of earthquakes within 30 km distance west of Saba, using data from the single stations at Saba, St. Eustatius, and St. Maarten. We applied the coincidence trigger on data from SABA, SEUS, and SMRT in search for similar events to the **M** 4.0 earthquake on 14 January 2008 and found a total of 25 earthquakes.

Geochronology suggests that the most recent eruption at Mt. Scenery took place about 400 yr ago, whereas at the Quill this was about 1600 yr ago (Roobol and Smith, 2004). Therefore, we started to apply and evaluate the coincidence trigger on data from the network on Saba, and this process will be extended to the waveform data from St. Eustatius in the near future. We used the coincidence trigger in ObsPy (Beyreuther *et al.*, 2010) with the previous settings on the BH data streams and found 1268 coincidence triggers for the network on Saba in the period 01 January 2017–01 April 2022. All these coincidence triggers were evaluated visually, and if an event was suspected, waveform data were analyzed using data from NA and adjacent networks. Through this procedure about 40 previously unnoticed earthquakes were identified, like the one East of Saba displayed in Figure 3.

The onset of a seismic phase is mainly determined by the source mechanism, subsurface medium characteristics (e.g., attenuation, dispersion, and scattering), the signal-to-noise ratio (SNR) at the recording site, and the characteristics of both the seismometer and the recording system. The sites in the NA network show relatively high seismic noise levels at frequencies above 1 Hz (de Zeeuw-van Dalfsen and Sleeman, 2018), most likely due to anthropogenic noise and wind. Such conditions, as well as the spatially sparse and small aperture configuration of the combined seismic networks in the region, are challenging for any automated system monitoring this region, making manual reviews indispensable. We aim for consistent and accurate determination of earthquake locations while doing these reviews, although the visual determination of phase arrival times may imply inconsistency and subjectivity, and thus affect the accuracy of phase picks (Diehl *et al.*, 2012). We try to minimize these effects by consistently following a procedure where all seismic analysts (a) apply the same filter (high pass at 0.5 Hz) to all traces prior to phase picking and (b) limit the contribution of seismic stations beyond 300 km distance to the analysis. Phase pick time residuals, defined as the difference between the observed and the calculated phase onset time, and their root mean square (rms) provide a measure for the accuracy of the inversion process. We usually do not accept phase pick time residuals beyond 0.5 s and aim for an rms less than 0.4 s.

RESULTS

The reviewed KNMI NA earthquake catalog is based on automatic detections by SeisComP as well as triggers from the coincidence trigger algorithm, which are manually reviewed within SeisComP on a daily basis. This catalog will become available in the near future. From 01 January 2017 to 07 June 2022, we detected and located 344 earthquakes in the region [65° W, 60° W] and [15° N, 20° N] (Fig. 4), with magnitudes ranging from 0.4 to 6. We manually located 241 earthquakes, of which 160 are within 150 km distance of Saba.

The seismicity in this region in this time frame is characterized by earthquakes that align in depth with the subduction zone. In Figure 5, we visually compare our catalog with 20 yr of

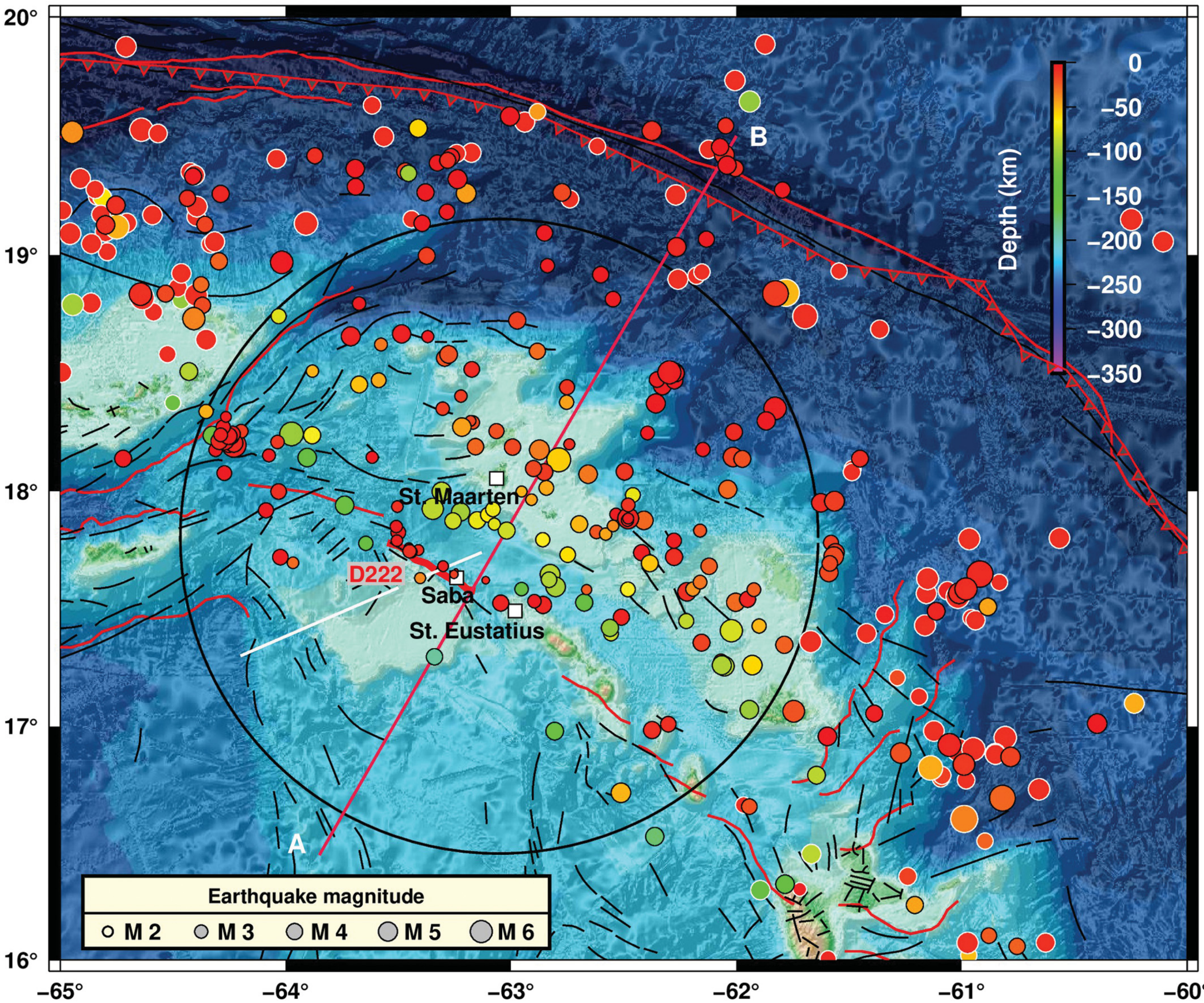

Figure 4. Earthquake epicenters detected by the NA network from 01 January 2017 to 07 June 2022, color coded by depth and sized according to magnitude. Circles with black borders represent (243) manually reviewed locations, whereas circles with white borders represent (103) automatic solutions. The large circle has a 150 km radius from the center of the NA network. Saba, St. Eustatius, and St. Maarten are indicated by white squares. Background shows a bathymetry map (GEBCO). Tectonic faults are represented by red lines (Styron *et al.*, 2020) and black lines (French and Schenk, 2004). D222 is a tectonic fault (thick red line) close to Saba, dipping to the northeast at about 70° (Global Earthquake Model [GEM]). The light gray line is a tectonic fault (Roobol and Smith, 2004). Line A–B indicates a depth profile across the subduction zone, as shown in Figure 5.

data in the ISC catalog, projected on the vertical plane of profile A–B (Fig. 4). The bulk data from the ISC provides a good reference for the seismicity distribution with depth in the region of the subduction slab. Our catalog does not show systematic outliers compared to the ISC. Around 50% of the earthquakes have a magnitude between 3 and 4 (Fig. 6).

From 01 January 2007 to 31 December 2016, the coincidence trigger detected 25 earthquakes. These shallow (5–10 km), magnitude 2.3–4 earthquakes were manually located west of Saba (Fig. 7). Most (22) occurred from 14 January 2008 to 23 March 2008, three more similar events were detected in the same region, in (1) July 2013 and (2) July 2014, having magnitudes from 2.6 to 3.1. All the 25 events occurred in the same region west of Saba as the 1992 swarm (Fig. 7), at similar depths (Fig. 8). Hence, seismicity within 30 km distance from Saba seems to be dominated by shallow (5–10 km depth) earthquakes aligning a tectonic fault striking west–southwest to east–northeast as identified by Roobol and Smith (2004).

Waveform data from SEUS for the **M** 3.6 earthquake near Saba in 2008 (Fig. 9a) show an emergent earthquake signal without clear *P* and *S* onsets. Recordings by SEUS from the other "similar" earthquakes in 2008, 2013, and 2014 show the same characteristic. A similar emergent onset is seen in the waveform data from SEUT and SEUG for the 2014

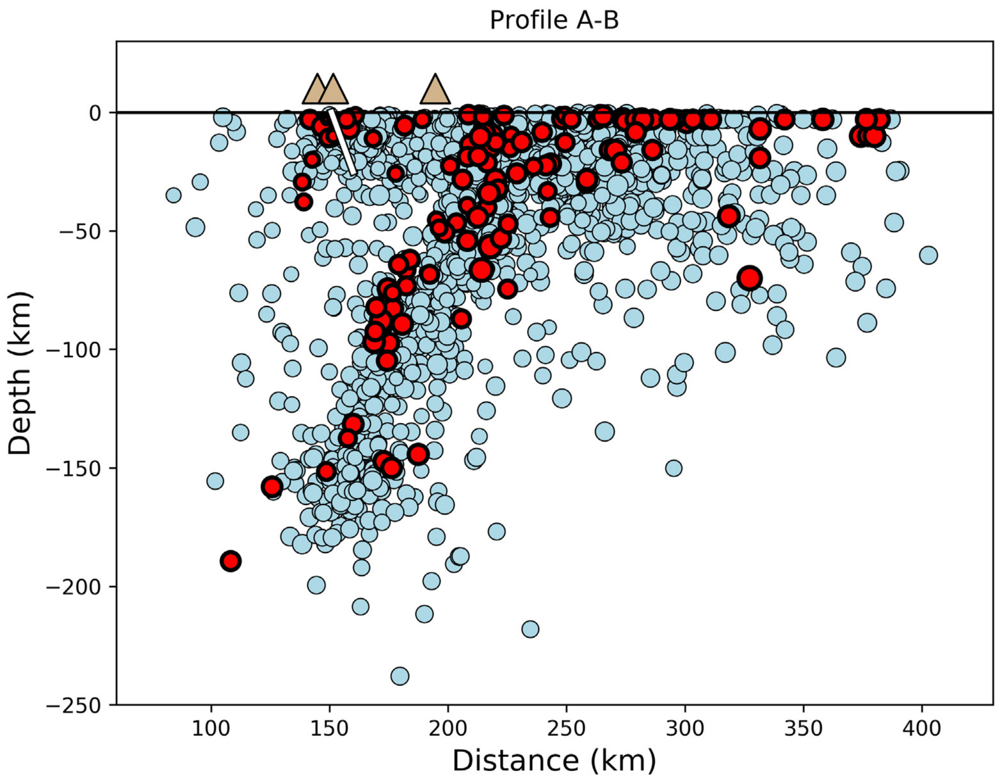

Figure 5. Earthquake hypocenters (circles with thick borders; KNMI, 01 January 2017–06 June 2022; circles with thin borders: International Seismological Center (ISC), 01 January 2000–01 January 2022) within 100 km distance from profile A–B (Fig. 4), mapped on the vertical plane. Note that the difference in number of earthquakes is mainly caused by the longer observation period for ISC. Triangles from left to right are the projection of Saba, St. Eustatius, and St. Maarten on the profile A–B. The dipping line is the projection of the 70° dipping fault D222 (Fig. 4) assuming a crustal depth of 27 km (Bie *et al.*, 2019). The color version of this figure is available only in the electronic edition.

earthquakes west of Saba. Waveform data of the same events for stations on Saba do show clear *P* and *S* wave arrivals.

Within a 30 km distance from Saba, between 2007 and 2017, ISC reports 47 earthquakes with magnitudes from 2.7 to 4.2, including the 11 earthquakes in 2008 mentioned previously. However, we could not confirm the occurrence and/or location of 32 reported earthquakes so close to Saba. In 16 cases, no earthquake signal was visible or detectable (Fig. 9b), and in eight cases the *S*–*P* phase difference at SABA was too large (>5 s) to explain an epicentral distance of less than 30 km. For three events, the phase arrival at SABA was later than at SEUS. In one case, no data for all three stations were available. In the remaining four cases, signals were visible with low SNRs and could not be processed accurately.

For about 87% of the reviewed events in 2017–2022, the rms is equal to or below 0.4 s (Fig. 6). As the rms depends on the number and distribution of stations (Husen and Hardebeck, 2010), this number does not give an indication of the error of the location. However, analysis of the time residuals may be useful to identify station-dependent biasing. These can then be added as station corrections to the inversion procedure to compensate for imperfections in the velocity model and thus to further improve the accuracy of the hypocenters (Bondár *et al.*, 2004). Table 2 shows the time residuals and their standard deviations for the *P*- and *S*-phase onsets at all NA stations. Except for SMRT all the stations show a positive bias in the average *P* residuals, ranging between 0.0 and 0.16 s; however, these are within the standard deviation of about 0.3 s. A positive bias in the *P* residual indicates a delay in travel time compared to the velocity model. For the *S* residuals, the average values are ranging from −0.13 to 0.05 s. The differences in numbers of phases between the stations also depend on the station operability.

The accuracy of a calculated earthquake location depends, amongst others, on the network layout like the number of stations, distance to the epicenter, and the azimuthal gap. The distribution of seismic stations in our region is strongly limited by the lack of land above sea level. For 96% of the earthquakes in the KNMI catalog, the azimuthal gap in the coverage of the contributing station is beyond 120°, which is important for getting accurate locations (Bondár *et al.*, 2004), with a mean of 222°. For 64% of the calculated origins, data from less than 10 stations were used, mainly because clear phase onsets were absent, or they were difficult to identify due to low SNR values, which also affects the location accuracy.

The proper way to represent the error in a hypocenter location is by the uncertainty ellipsoid. In our dataset of reviewed earthquakes, the uncertainty ellipsoids show that the largest uncertainties in the locations are oriented with directional azimuths of about 30° (Fig. 10a). This is more or less perpendicular to the elongated distribution of seismic stations on the islands along the subducting arc (Fig 1). About 90% of the horizontal uncertainty, expressed by the major axis length of the confidence ellipsoid, are within 35 km. The error in depth is less than 10 km for 55% of the earthquakes and less than 20 km for 82%.

We compare the earthquake catalogs from KNMI and USGS in terms of epicentral difference (distance and azimuth; Fig. 10). The distribution of these differences is oriented in the

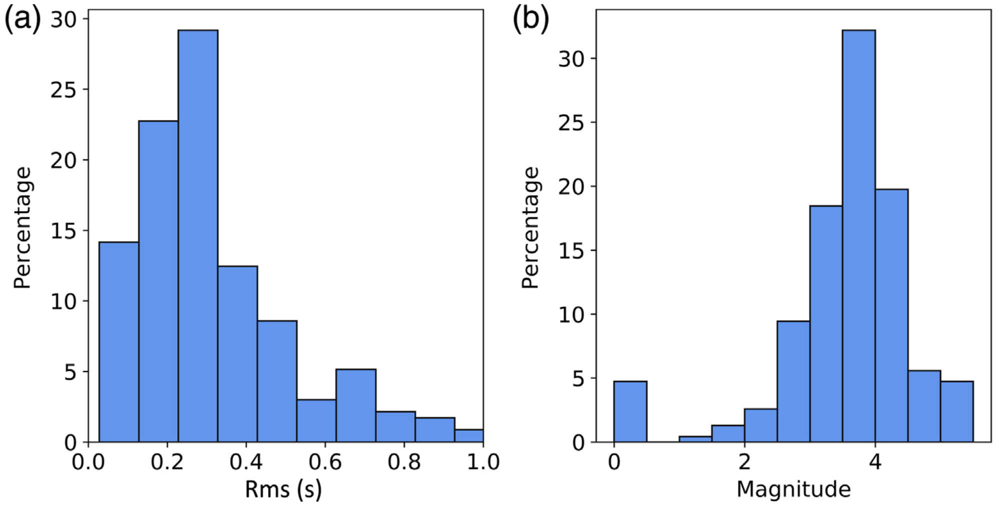

Figure 6. (a) Distribution of root mean square (rms) of time residuals of 160 manually reviewed earthquakes within 150 km distance from Saba from 01 January 2017 to 07 June 2022. (b) Magnitude distribution of these earthquakes. The color version of this figure is available only in the electronic edition.

same direction as the uncertainty ellipsoids. About 85% of the horizontal distances between KNMI and USGS epicenters are within the uncertainty ellipses of our catalog.

DISCUSSION

The NA seismic network in the Caribbean Netherlands detects previously unnoticed earthquakes down to magnitude 0.4 within 150 km distance from Saba. The network, therefore, significantly contributes to knowledge of seismicity in this region. This will open new research possibilities to identify active tectonic faults and to better quantify their physical properties (e.g., dip, strike). For example, we located a number of earthquakes west of Saba, close to fault D222 (Fig. 4). The GEM (Global Earthquake Model Foundation) fault database mentions that the location of this fault is not constrained by any topography or bathymetry (Feuillet *et al.*, 2011). Seismic observations can help identify the fault location, type, and mechanism.

Within the radius of 150 km two areas seem to show spatial clustering of shallow earthquakes, around (64.4° W, 18.2° N) and (62.6° W, 17.8° N). Continued monitoring over time is needed to investigate the cause of these clusters in more detail. Clustering can be due to, for example, active faulting or sustained movement of fluids in the crust (Halpaap *et al.*, 2019). The increased data availability will help shed light on the origin of the observed clustering.

Usual "background" seismicity in the region aligns in depth with the subduction zone (Fig. 5), down to 200–300 km. Earthquakes from two swarms (1992 and 2008) in the direct vicinity of Saba are shallower (~10 km depth) and seem to follow two local faults: one parallel (D222; Figs. 4, 5, 7) and one oblique (light gray line; Figs. 4, 7) to the subduction zone. The former is described in the GEM catalog; the latter west–southwest to east–northeast-striking fault was previously identified by Roobol and Smith (2004). Compared with the swarm in 1992, the epicenters of the 2008 swarm align more prominent with the west-southwest–east-northeast-striking fault. Availability of more data with higher accuracy from improved instruments and the use of modern analysis tools could contribute to this difference. Continued monitoring with the updated NA network is expected to deliver more detailed locations and source mechanisms of future swarms. Further research is required to investigate the cause of the emergent onset in the recordings by the seismometers at St. Eustatius, which could possibly be related to the source mechanism or the inhomogeneous velocity structure beneath Mt. Scenery.

TABLE 2
Number of (Manually Picked) *P* and *S* Phases for Each NA Station in Operation for a Minimum of One Year, the Mean Time Residuals, and Their Standard Deviation

Station Code	Number of *P* Phases	Mean *P* Residual (s)	St. Dev. of *P* Residual (s)	Number of *S* Phases	Mean *S* Residual (s)	St. Dev. of *S* Residual (s)
SABA	167	0.08	0.30	78	0.05	0.28
SABQ	125	0.0	0.30	52	−0.12	0.29
SABW	210	0.11	0.26	110	0.0	0.23
SABY	105	0.16	0.30	76	0.05	0.29
SEUG	146	0.08	0.26	86	0.0	0.24
SEUS	110	0.06	0.31	81	−0.13	0.27
SEUT	168	0.11	0.27	85	0.05	0.26
SMRT	187	−0.05	0.28	149	−0.10	0.34

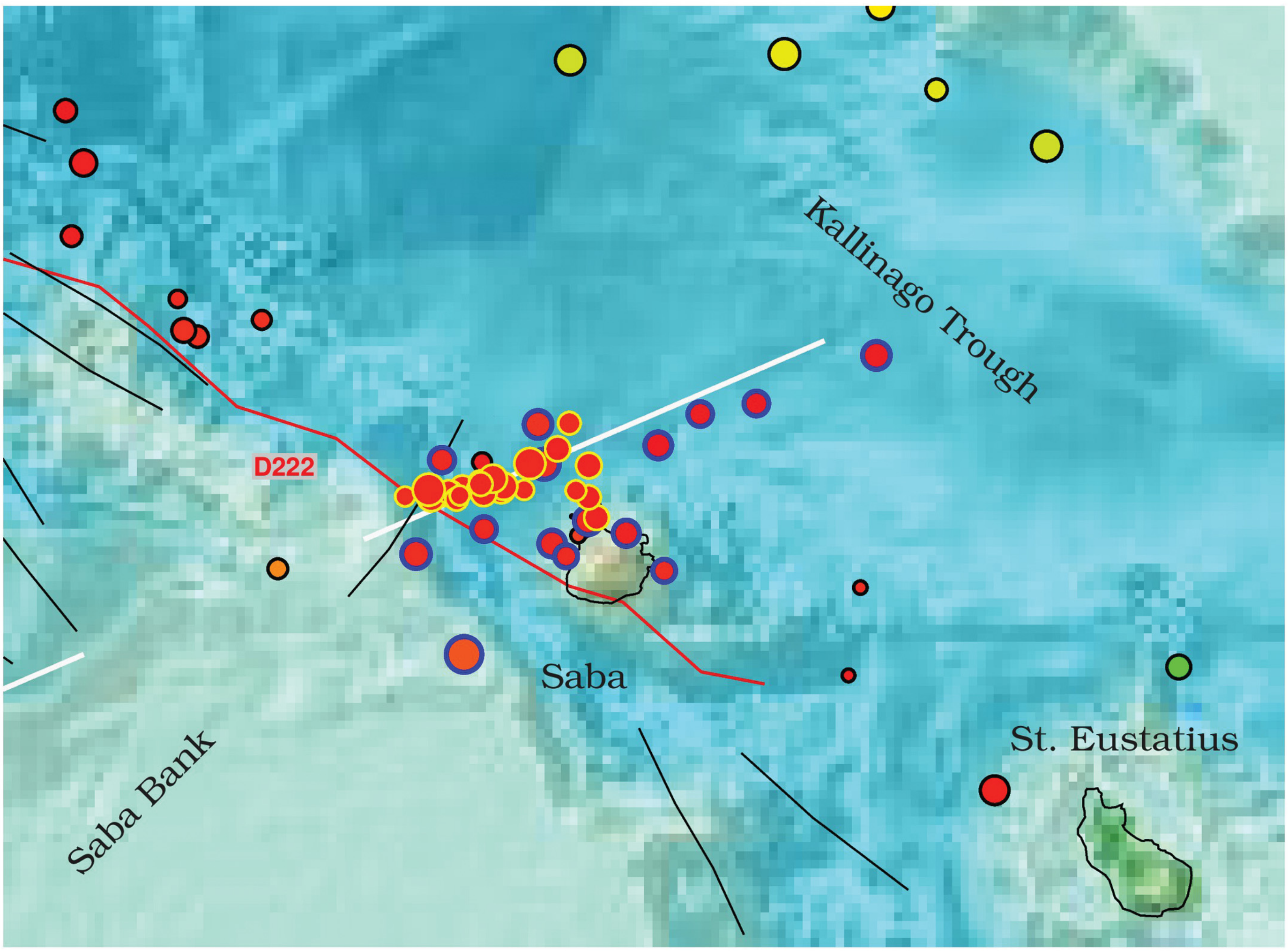

Figure 7. Earthquake swarms epicenters around Saba. Circles with black borders represent the manually reviewed locations for the NA detections between 01 January 2017 and 07 June 2022, color coded by depth and sized according to magnitude as in Figure 4. The swarm of earthquakes in 1992 is represented by the circles with blue borders. Circles with yellow borders are the epicenters of the swarm of earthquakes in 2008, and three earthquakes in 2013 and 2014 (see Results section). Tectonic faults are represented as in Figure 4.

The contribution of seismic phase onset times to centers like USGS and ISC are important for building up a comprehensive catalog. Reliable phase picks will help those data centers to determine hypocenters with improved accuracy. Currently data from NA stations SABA, SABQ, SABW, SABY, SEUG, SEUS, SEUT, and SMRT are available in real time for monitoring purposes. We encourage inclusion of these stations in the monitoring by USGS, UPR, and UWI-SRC. We also noticed a number of ISC reported earthquakes where the absence of phase picks of NA stations helped us to identify wrongly or falsely reported hypocenters. The absence of any detectable signal at a seismometer closer to the hypocenter than those used to calculate the hypocenter is valuable information that is usually not used in the inversion process. Therefore, the absence of seismic phases at stations where one may expect these may help to further improve the accuracy in earthquake catalogs.

The possible positive bias in the *P* residual at all seismometers on Saba and St. Eustatius indicates a consistent delay in *P*-wave travel time. A positive delay could be interpreted as caused by lower velocities in material of higher temperature or by the existence of a thin, shallow, low-velocity layer (Lesage *et al.*, 2018). Our current *P* velocity 1D model is not optimal to represent the true, complex seismic velocity structure with large lateral velocity inhomogeneities in the subduction zone. Also the seismic velocity structure beneath volcanoes Mt. Scenery and The Quill is more complex than the layered IASPEI91 model, and could contribute to the possible positive bias in the *P* residuals. Lesage *et al.* (2018) have proposed a generic *P*- and *S*-wave velocity model for the first 500 m of andesitic and basaltic volcanoes to accommodate for very low velocities at the surface and a strong velocity increase at shallow depth. Further testing with this model and the unified velocity model proposed by Bie *et al.* (2019) is required to assess the effect of the velocity model on both time residuals and location accuracy.

Usually, accuracy of epicenters of 5 km with a 95% confidence level can be obtained for crustal earthquakes inside

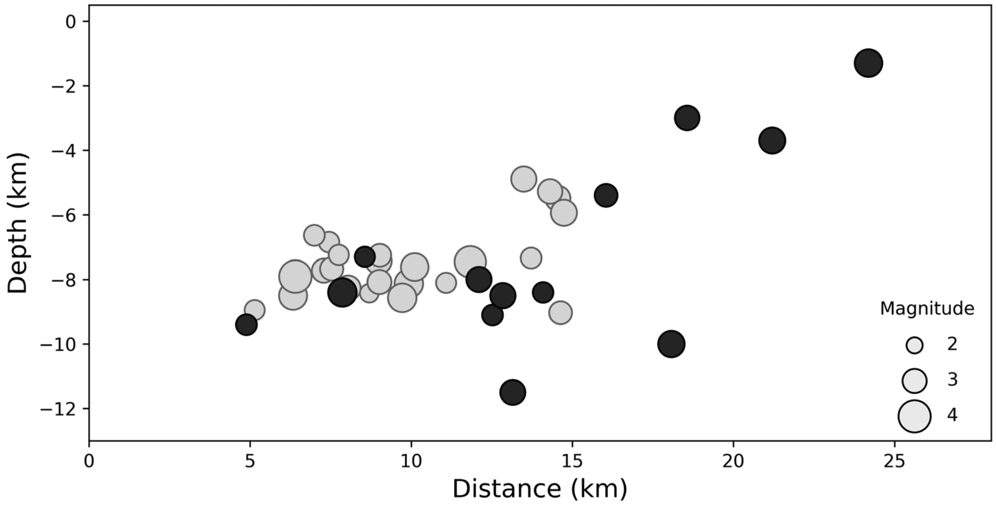

Figure 8. Earthquake hypocenters (gray; swarm 2008, 2013, and 2014; black: swarm 1992) within 7 km distance from the west–southwest to east–northeast-striking tectonic fault northwest of Saba (Fig. 7), mapped on the vertical plane.

dense, local networks (Bondár *et al.*, 2004) when data (1) are available from at least 10 stations within 250 km, (2) have an azimuthal gap of less than 120°, and (3) of one or more stations are within 30 km distance of the epicenter. The current distribution of seismic stations along the volcanic arc makes that these criteria are not met for most of the earthquakes in the region of this study. In particular, the elongated distribution along the island arc causes the azimuthal gap of 120° to be exceeded in 97% of the cases. Besides, only a few seismic stations from the adjacent networks are within 250 km distance. In 67% of the events less than 10 stations contributed to the origin. These limiting factors all augment the inaccuracy of the locations and may explain the relatively large horizontal errors in our catalog. In addition, due to the overall elongated configuration of the networks in the region into the southeast to northwest direction, the aperture of the network is small in the perpendicular direction. Therefore, the largest epicentral uncertainties are in the northeast to southwest direction (Havskov *et al.*, 2012). Mislocations of several tens of kilometers are not uncommon in subduction zones with large lateral velocity inhomogeneities like a subduction zone and are even larger for a network with limited azimuthal coverage (Havskov *et al.*, 2012). Ways to improve the accuracy in calculated earthquake locations are the deployment of stations close to and above the hypocenter zone as well as the use of location algorithms that are robust to errors in both the velocity model and in phase onset times (Lomax and Savvaidis, 2019). Obviously, the deployment of (permanent) ocean-bottom seismometers (Cabieces *et al.*, 2020) would decrease the azimuthal and distance gaps throughout the overall network, and thus be beneficial for improving both detection capability and location accuracy of earthquakes. Finally, relative location methods (e.g., Waldhauser and Ellsworth, 2000) may improve the interevent accuracy of the locations; however, these procedures also depend on good station and seismic path coverage (Lomax and Savvaidis, 2022). The development of new, advanced techniques such as NonLinLoc Source Specific Station Traveltime (NLL-SSST)-coherence relocation (Lomax and Savvaidis, 2022) are intriguing to apply, as they may enable precise, relative earthquake relocation with sparse networks.

Besides monitoring tectonic earthquakes, a challenge for our monitoring system is the detection, identification, and locating of volcanic earthquakes. The absence of recordings of known volcanic earthquakes at Mt. Scenery and/or The Quill, however, prevents early recognition of this kind of signals and requires manual review per event. Often volcanic activity starts with the occurrence of transient volcanoseismic signals at shallow to intermediate depths with clear *P*- and *S*-phase onsets (Zobin, 2017). Therefore, we expect that our system will detect such tectonic-like earthquakes at an early stage. The complex subsurface structure of the volcano, however, may also cause strong interferences of waves due to scattering making it difficult to clearly distinguish *P* and *S* phases. Figure 11 shows an example of a seismic signal, with seismic energy up to more than 30 Hz, recorded and detected by SABN where no distinct *S* phase can be observed.

Advanced systems for earthquake signal detection and recognition are becoming more and more advantageous for automated detection and classification of the various (seismic) signals in a continuously growing dataset. For example, the coincidence trigger provides a large number of detections that do not resemble tectonic earthquake signals. Volcano seismology deviates from conventional earthquake seismology from the physics of the source to the methods to analyze the signals (Wassermann, 2012). In volcano seismology signals may vary between tectonic-like, transient earthquake signals to more continuous signals known as tremors. Systematic research on the detections in our data may help to find similarities and common features in the data that we currently are not aware of. Neural networks (Trani *et al.* 2022), the Volcano-Independent Volcano-Seismic Recognition system (Cortés *et al.*, 2021), or the Adaptive-Window Volcanic Event Selection Analysis Module (Fenner *et al.*, 2022) can help to better understand the various seismic signals recorded on

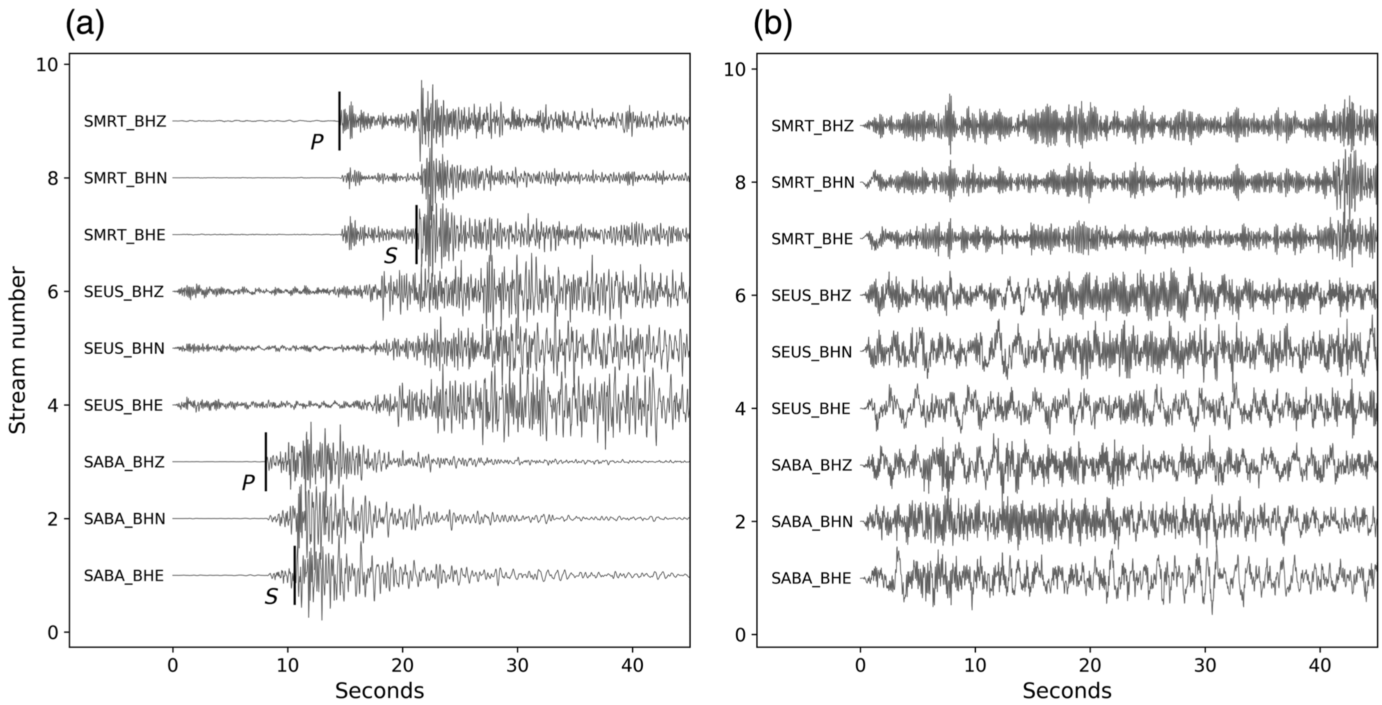

Figure 9. Recordings by SMRT, SEUS, and SABA for two reported earthquakes in the ISC catalog. (a) 14 January 2008 14:32:59, **M** 3.6, depth 43 km and (b) 25 August 2014 05:24:50, **M** 3.1, depth 136 km. All traces are scaled to their maximum amplitude. Manual *P* and *S* picks are indicated with the vertical lines.

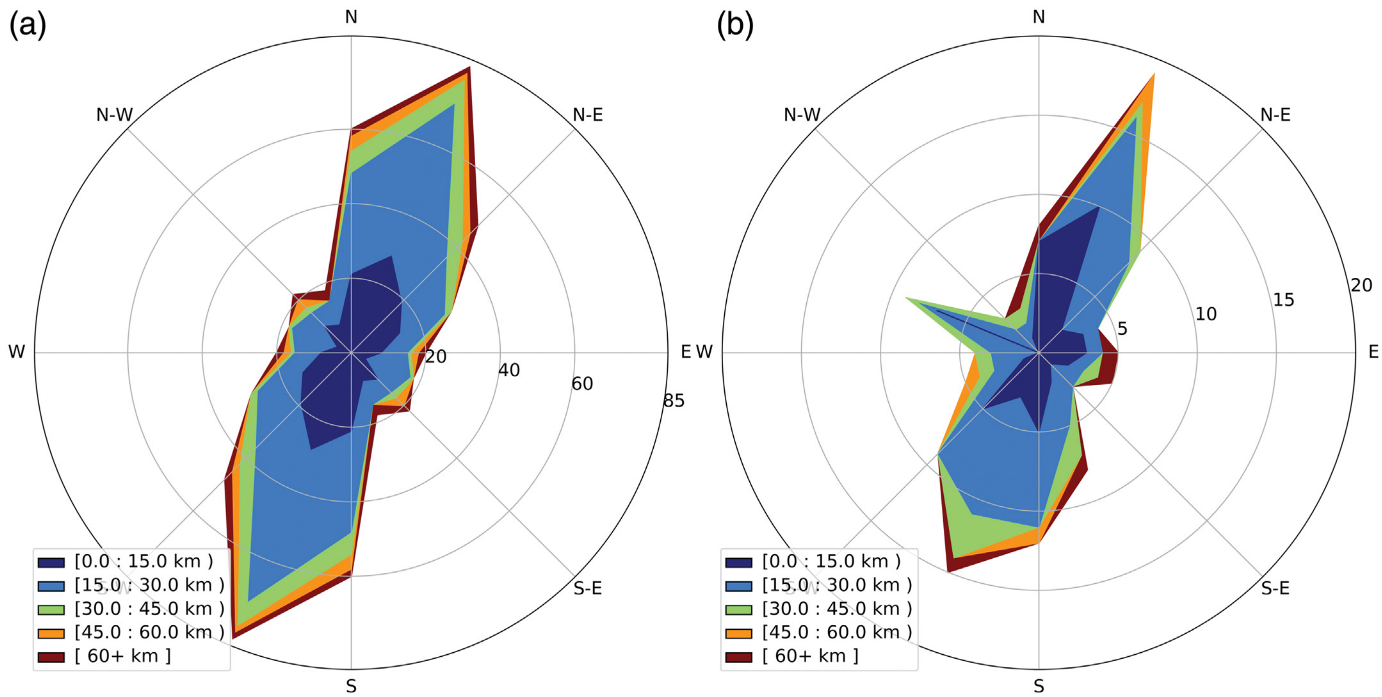

Figure 10. (a) Windrose diagram showing the distribution of azimuth and major axis length of the confidence ellipsoid for all earthquake origins in the KNMI catalog. (b) Windrose diagram representing the differences in azimuth and distance between earthquakes commonly detected by USGS and KNMI (01 January 2017–07 June 2022). Colors indicate the epicentral difference in kilometers as a function of azimuth. Radii of the circles indicate percentage of occurrence.

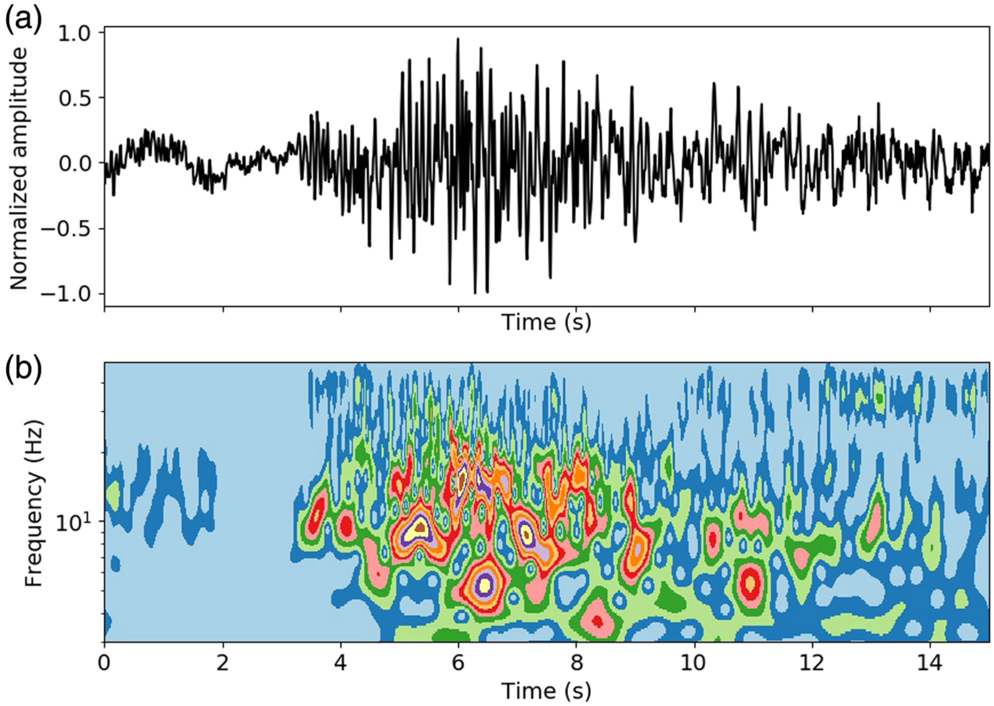

Figure 11. (a) Seismogram and (b) the corresponding spectrogram recorded at the north component of SABN (04 June 2022 18:50:50) at 100 samples per second. The spectrogram is calculated using the *S* transform to optimize time resolution at all frequencies. The color version of this figure is available only in the electronic edition.

Mt. Scenery and The Quill, and prepare our monitoring system to detect and classify both volcanic and tectonic earthquakes.

CONCLUSION

Data from the NA seismic network in the Caribbean Netherlands reveal previously unnoticed earthquakes down to magnitude 0.4 within 150 km distance from Saba. The use of the coincidence trigger has proven to be important to detect earthquakes with a few stations only. Locating earthquakes in the area of interest can be done with a limited accuracy of tens of kilometers due to the complex seismic velocity structure in the subduction zone, the small aperture of the seismic networks in the northeast–southwest direction, and the limited number of stations. Within these errors our catalog compares well with the USGS catalog. The network, therefore, significantly contributes to the monitoring and knowledge of seismicity in the region.

Within the current region of interest the seismicity is characterized by (a) earthquakes that align in depth with the subduction zone and (b) shallow (~10 km) earthquakes near Saba along tectonic faults parallel and oblique to the subduction zone. The presence of the expanded NA network enhances the detection capability around Saba, St. Eustatius, and St. Maarten and will enable detailed studies of future earthquake swarms.

DATA AND RESOURCES

Earthquake data from the U.S. Geological Survey (USGS) and International Seismological Center (ISC) were retrieved using the International Federation of Digital Seismograph Networks (FDSN) standardized webservice (https://earthquake.usgs.gov/fdsnws/event/1/query and http://www.isc.ac.uk/fdsnws/event/1/query, both last accessed June 2022). Bathymetry data were obtained from General Bathymetric Chart of the Oceans (GEBCO; https://download.gebco.net/). Some of the plots were made using the Generic Mapping Tools (GMT) version 6.0.0 (www.soest.hawaii.edu/gmt; Wessel *et al.*, 2019). Tectonic faults in the Caribbean region were obtained from the GEM (Global Earthquake Model Foundation) fault database (https://www.globalquakemodel.org/). Seismic noise characteristics of the NA stations can be found at http://www.orfeus-eu.org/data/odc/quality/ppsd/. The Caribbean Netherlands Seismic Network is available at www.fdsn.org/networks/detail/NA. The Netherlands Seismic and Acoustic Network is available at www.fdsn.org/networks/detail/NL. SeisComP software is available at www.gempa.de. All websites were last accessed in November 2022.

DECLARATION OF COMPETING INTERESTS

The authors declare that there are no conflict of interests recorded.

ACKNOWLEDGMENTS

Building up and maintaining a remote seismic network does not come without the help of many. The authors work would not have been possible without the continued support from the governments of Saba and St. Eustatius, especially Jonathan Johnson, Shamara Amalia Nicholson, Tim Muller, Lune Zijnen, Alida Francis, Claudia Toet, Malvern Dijkshoorn, and Edris Bennett. The authors are grateful to the continuous support from Tim van Oosteren, Sonya Johnson, and their colleagues from Satel, and Fernando Simmons, Maryteresse Redan, Adriaan Schmidt, and their colleagues from Eutel. The authors thank J. Isaac and Lucien Pinas from the Meteorological Department of St. Maarten for their support to keep seismometer SMRT up and running throughout the years. The authors thank George and Shelly Works for their support to deploy seismic station SEUG on their premises. In particular, their KNMI colleagues Hendrik-Jan Bosch, Belmin Kuc, and Andreas Krietemeyer are thanked a lot for their work and help with logistics before and during the installation of the most recent seismometers: SEUH, SABN, and SEUB. In addition, the local support from

Sebastiaan Keijzer and Rick van Eeden is greatly appreciated. The authors learned a lot about volcano seismology from their colleagues at the regional volcano observatories in Guadeloupe, Montserrat, and Trinidad. Finally, the authors thank Bernard Dost and the two anonymous reviewers for their valuable feedback and input to improve this article.

REFERENCES

Albuquerque Seismological Laboratory/U.S. Geological Survey (ASL/USGS) (1988). Global Seismograph Network - IRIS/USGS [Data set], *International Federation of Digital Seismograph Networks*, doi: 10.7914/SN/IU.

Albuquerque Seismological Laboratory/U.S. Geological Survey (ASL/USGS) (2006). Caribbean USGS Network [Data set], *International Federation of Digital Seismograph Networks*, doi: 10.7914/SN/CU.

Ambeh, W. B., and L. L. Lynch (1995). The earthquake sequence of June 1992 near Saba, West Indies, *Tectonophysics* **246,** 225–243, doi: 10.1016/0040-1951(94)00254-7.

Anglade, A., A. Lemarchand, J.-M. Saurel, V. Clouard, and M.-P. Bouin (2015). Significant technical advances in broadband seismic stations in the Lesser Antilles, in *Advances in Geosciences*, Vol. 40, European Geosciences Union, 43–50, doi: 10.5194/ADGEO-40-43-2015.

Beyreuther, M., R. Barsch, L. Krischer, T. Megies, Y. Behr, and J. Wassermann (2010). ObsPy: A python toolbox for seismology, *Seismol. Res. Lett.* **81,** 530–533.

Bie, L., A. Rietbrock, S. Hicks, R. Allen, J. Blundy, V. Clouard, J. Collier, J. Davidson, T. Garth, and S. Goes (2019). Along-arc heterogeneity in local seismicity across the lesser antilles subduction zone from a dense ocean-bottom seismometer network, *Seismol. Res. Lett.* **91,** 237–247, doi: 10.1785/0220190147.

Bondár, I., S. C. Myers, E. R. Engdahl, and E. A. Bergman (2004). Epicentre accuracy based on seismic network criteria, *Geophys. J. Int.* **156,** no. 3, 483–496, doi: 10.1111/j.1365-246X.2004.02070.x.

Bratt, S., and W. Naggy (1991). The LocSAT Program, Science Applications International Corporation (SAIC), San Diego, California.

Cabieces, R., E. Buforn, S. Cesca, and A. Pazos (2020). Focal parameters of earthquakes offshore Cape St. Vincent using an amphibious network, *Pure Appl. Geophys.* **177,** 1761–1780, doi: 10.1007/s00024-020-02475-3.

Cortés, G., R. Carniel, P. Lesage, A. M. Mendoza, and I. Della Lucia (2021). Practical volcano-independent recognition of seismic events: VULCAN.ears Project, *Front. Earth Sci.* **8,** doi: 10.3389/feart.2020.616676.

de Zeeuw-van Dalfsen, E., and R. Sleeman (2018). A permanent, real-time monitoring network for the volcanoes mount scenery and the Quill in the Caribbean Netherlands, *Geosciences* **8,** no. 9, doi: 10.3390/geosciences8090320.

Diehl, T., E. Kissling, and P. Bormann (2012). Tutorial for consistent phase picking at local to regional distances, in New Manual of Seismological Observatory Practice 2 (NMSOP-2), P. Bormann (Editor), Deutsches GeoForschungsZentrum GFZ, Potsdam, Germany, 1–21, doi: 10.2312/GFZ.NMSOP-2_IS_11.4.

Dondin, F. J.-Y., L. Lynch, L. C. Ramsingh, G. A. Ryan, I. Papadopoulous, D. Rueppel, E. P. Joseph, J. L. Latchman, R. E. A. Robertson, N. Nath, *et al.* (2019). The University of the West Indies-Seismic Research Centre volcano monitoring network: Evolution since 1953 and challenges in maintaining a state-of-the-art network in a small island economy, *Geosciences* **9,** doi: 10.3390/geosciences9020071.

Fenner, D., G. Rümpker, W. Li, M. Chakraborty, J. Faber, J. Köhler, H. Stöcker, and N. Srivastava (2022). Automated seismo-volcanic event detection applied to Stromboli (Italy), *Front. Earth Sci.* **10,** doi: 10.3389/feart.2022.809037.

Feuillet, N., F. Beauducel, and P. Tapponnier (2011). Tectonic context of moderate to large historical earthquakes in the Lesser Antilles and mechanical coupling with volcanoes, *J. Geophys. Res.* **116,** no. B10, doi: 10.1029/2011JB008443.

French, C. D., and C. J. Schenk (2004). Faults of the Caribbean Region (flt6bg), *U.S. Geol. Surv. Data Release* [Data set], doi: 10.5066/P9GVH21Y.

Halpaap, F., S. Rondenay, A. Perrin, S. Goes, L. Ottemöller, H. Austrheim, R. Shaw, and T. Eeken (2019). Earthquakes track subduction fluids from slab source to mantle wedge sink, *Sci. Adv.* **5,** no. 4, eaav7369, doi: 10.1126/sciadv.aav7369.

Havskov, J., L. Ottemöller, A. Trnkoczy, and P. Bormann (2012). Seismic Networks, in *New Manual of Seismological Observatory Practice 2 (NMSOP-2)*, P. Bormann (Editor), Deutsches GeoForschungsZentrum GFZ, Potsdam, Germany, 1–65, doi: https://doi.org/10.2312/GFZ.NMSOP-2_ch8.

Husen, S., and J. L. Hardebeck (2010). Earthquake location accuracy, *Community Online Resource for Statistical Seismicity Analysis*, doi: 10.5078/corssa-55815573.

Institut de physique du globe de Paris (IPGP) (2008). GNSS, seismic broadband and strong motion permanent networks in West Indies, Institut de physique du globe de Paris (IPGP), Université de Paris, doi: 10.18715/antilles.WI.

Institut de physique du globe de Paris (IPGP) and École et Observatoire des Sciences de la Terre de Strasbourg (EOST) (1982). GEOSCOPE, French Global Network of broadband seismic stations, Institut de physique du globe de Paris (IPGP), Université de Paris, doi: 10.18715/GEOSCOPE.G.

Kennett, B. L. N., and E. R. Engdahl (1991). Travel times for global earthquake location and phase association, *Geophys. J. Int.* **105,** 429–465, doi: 10.1111/j.1365-246X.1991.tb06724.x

KNMI (2006). Caribbean Netherlands Seismic Network, NA, Royal Netherlands Meteorological Institute (KNMI) [Data set], doi: 10.21944/dffa7a3f-7e3a-3b33-a436-516a01b6af3f.

Lesage, P., M. J. Heap, and A. Kushnir (2018). A generic model for the shallow velocity structure of volcanoes, *J. Volcanol. Geotherm. Res.* **356,** 114–126, doi: 10.1016/j.jvolgeores.2018.03.003.

Lindsay, J. M., and R. E. A. Robertson (2018). Integrating volcanic hazard data in a systematic approach to develop volcanic hazard maps in the Lesser Antilles, *Front. Earth Sci.* **6,** doi: 10.3389/feart.2018.00042.

Lomax, A., and A. Savvaidis (2019). Improving absolute earthquake location in west Texas using probabilistic, proxy ground-truth station corrections, *J. Geophys. Res.* **124,** 11,447–11,465, doi: 10.1029/2019JB017727.

Lomax, A., and A. Savvaidis (2022). High-precision earthquake location using source-specific station terms and inter-event waveform similarity, *J. Geophys. Res.* **127,** e2021JB023190, doi: 10.1029/2021JB023190.

Massin, F., V. Clouard, I. Vorobieva, F. Beauducel, J.-M. Saurel, C. Satriano, M.-P. Bouin, and D. Bertil (2021). Automatic picking and probabilistic location for earthquake assessment in the Lesser Antilles subduction zone (1972–2012), *Compt. R. Géosci.* **353,** no. S1, 187–209, doi: 10.5802/crgeos.81.

Proenza, X., and G. Maul (2010). Tsunami hazard and total risk in the Caribbean basin, *Sci. Tsunami Hazards* **29**.

Roobol, M., and A. Smith (2004). *Volcanology of Saba and St. Eustatius, Northern Lesser Antilles*, Koninklijke Nederlandse Akademie van Wetenschappen, Amsterdam, The Netherlands.

Sleeman, R., and E. de Zeeuw-van Dalfsen (2020). Cross-correlation analysis of long-term ambient seismic-noise recordings in the Caribbean Netherlands to monitor the volcanoes on Saba and St. Eustatius, *Bull. Seismol. Soc. Am.* **110,** 2541–2558, doi: 10.1785/0120200011.

Strollo, A., D. Cambaz, J. Clinton, P. Danecek, C. P. Evangelidis, A. Marmureanu, L. Ottemöller, H. Pedersen, R. Sleeman, K. Stammler, *et al.* (2021). EIDA: The European Integrated Data Archive and Service Infrastructure within ORFEUS, *Seismol. Res. Lett.* **92,** no. 3, 1788–1795, doi: 10.1785/0220200413.

Styron, R., J. García-Pelaez, and M. Pagani (2020). CCAF-DB: the Caribbean and Central American active fault database, *Nat. Hazards Earth Syst. Sci.* **20,** 831–857, doi: 10.5194/nhess-20-831-2020.

Trani, L., G. A. Pagani, J. P. Pereira Zanetti, C. Chapeland, and L. Evers (2022). DeepQuake—An application of CNN for seismo-acoustic event classification in The Netherlands, *Comp. Geosci.* **159,** doi: 10.1016/j.cageo.2021.104980.

University of Puerto Rico (1986). Puerto Rico Seismic Network & Puerto Rico Strong Motion Program [Data set], *International Federation of Digital Seismograph Networks*, doi: 10.7914/SN/PR.

Waldhauser, F., and W. L. Ellsworth (2000). A double-difference earthquake location algorithm: Method and application to the Northern Hayward Fault, California, *Bull. Seismol. Soc. Am.* **90,** no. 6, 1353–1368, doi: 10.1785/0120000006.

Wassermann, J. (2012). Volcano seismology, in *New Manual of Seismological Observatory Practice 2 (NMSOP-2)*, P. Bormann (Editor), Deutsches GeoForschungsZentrum GFZ, Potsdam, Germany, 1–77, doi: 10.2312/GFZ.NMSOP-2_ch13.

Wessel, P., J. F. Luis, L. Uieda, R. Scharroo, F. Wobbe, W. H. F. Smith, and D. Tian (2019). The Generic Mapping Tools version 6, *Geochem. Geophys. Geosys.* **20,** 5556–5564, doi: 10.1029/2019GC008515.

Zimmerman, T., M. B. Shen-Tu, K. Shabestari, and M. Mahdyiar (2022). A comprehensive hazard assessment of the Caribbean Region, *Bull. Seismol. Soc. Am.* **112,** 1120–1148, doi: 10.1785/0120210157.

Zobin, V. M. (2017). *Introduction to Volcanic Seismology*, Third Ed., Elsevier, Amsterdam, Netherlands, doi: 10.1016/C2015-0-00304-5.

Manuscript received 29 June 2022
Published online 23 November 2022